

THE EVOLUTIONARY STATUS OF CLUSTERS OF GALAXIES AT $Z \sim 1$

Holland Ford¹, Marc Postman², J. P. Blakeslee¹, R. Demarco¹, M. J. Jee¹, P. Rosati⁴, B. P. Holden³, N. Homeier¹, G. Illingworth³, R. L. White²

¹*Johns Hopkins University, Baltimore, MD, USA* ²*Space Telescope Science Institute, Baltimore, MD, USA* ³*Lick Observatory, University of California, Santa Cruz, CA 95064* ⁴*Karl-Schwarzschild-Strasse 2, D-85748 Garching, Germany*

Abstract Combined HST, X-ray, and ground-based optical studies show that clusters of galaxies are largely "in place" by $z \sim 1$, an epoch when the Universe was less than half its present age. High resolution images show that elliptical, S0, and spiral galaxies are present in clusters at redshifts up to $z \sim 1.3$. Analysis of the CMDs suggest that the cluster ellipticals formed their stars several Gyr earlier, at $z \gtrsim 3$. The morphology–density relation is well established at $z \sim 1$, with star-forming spirals and irregulars residing mostly in the outer parts of the clusters and E/S0s concentrated in dense clumps. The intracluster medium has already reached the metallicity of present-day clusters. The distributions of the hot gas and early-type galaxies are similar in $z \sim 1$ clusters, indicating both have largely virialized in the deepest potentials wells.

In spite of the many similarities between $z \sim 1$ and present-day clusters, there are significant differences. The morphologies revealed by the hot gas, and particularly the early-type galaxies, are elongated rather than spherical. We appear to be observing the clusters at an epoch when the sub-clusters and groups are still assembling into a single regular cluster. Support for this picture comes from CL0152 where the gas appears to be lagging behind the luminous and dark mass in two merging sub-components. Moreover, the luminosity difference between the first and second brightest cluster galaxies at $z \sim 1$ is smaller than in 93% of present-day Abell clusters, which suggests that considerable luminosity evolution through merging has occurred since that epoch. Evolution is also seen in the bolometric X-ray luminosity function.

Keywords: Clusters of Galaxies, Cluster Evolution, Galaxy Evolution, High Redshift

1. Introduction

The Advanced Camera for Surveys (ACS) IDT is using the new capabilities of the ACS (Ford et al. 2002) to answer fundamental questions about clusters and cluster galaxies at redshifts $z \sim 1$, an epoch when they are approximately half the age of the Universe. Our goals include constraining the formation ages

and the SF history of early-type galaxies, measuring the fundamental properties of cluster galaxies (e.g. structure, morphology, and luminosity) and their relationships within the clusters, measuring the evolution of cluster and galaxy characteristics from $z \sim 1$ to the present, and investigating the assembly of the brightest cluster galaxies. We also aim to establish links between clusters at $z \sim 1$ and proto-clusters at $z \sim 2$ to 5 (Miley et al. 2004), though this will not be discussed here. In this paper we describe the results to date from our ongoing study of eight clusters at $z \sim 1$. In section 3 we discuss CL1252 and CL0152 in detail, the two clusters where our analysis has progressed furthest. In subsequent sections we discuss and compare properties of the entire sample, and then end with a discussion of the evolutionary status of the clusters.

2. Cluster Selection and Cluster Properties

Five of the clusters in our program were initially identified from the ROSAT Deep Cluster Survey (Rosati et al. 1998; RDCS), one from the Einstein Extended Medium Sensitivity Survey (Gioia & Luppino 1994; MS1054), and two from a Palomar deep near-infrared photographic survey (CL1604+4304 & CL1604 +4321; Gunn et al. 1986). The reality of the clusters has been confirmed by extensive spectroscopy with ground based telescopes. The properties of the clusters and their ACS observations are summarized in Table 1. The number of spectroscopically confirmed galaxies in each cluster is in parentheses in column 2. The velocity dispersions in column 3 are in the clusters' rest frames. The age of the Universe T_z at redshift z assumes $h = 0.7$, $\Omega_m = 0.30$, $\Omega_\Lambda = 0.70$, giving $T_0 = 13.47$ Gyr today, the cosmology we use throughout this paper unless stated otherwise.

Table 1. Properties of High Redshift Clusters Observed with ACS.

Cluster	Redshift ^a T_z (Gyr)	Rest Frame Vel. Dispersion	X-ray Lum. (10^{44} ergs s^{-1})	Filters ^b	Total Orbits
MS1054	0.831(143) 6.5	1112	23.3	V,i,z	24
CL0152	0.837 (102) 6.5	1632 ^c	7.8	r,i,z	24
CL1604+4304	0.897 (22) 6.2	1226	2.0	V,I	4
CL1604+4321	0.924 (44) 6.1	935	<1.2	V,I	4
CL0910	1.101 (10) 5.4	N/A	1.5	i,z	8
CL1252	1.237 (36) 4.9	760 ^d	2.5	i,z	32
CL0848-A,B	1.265 (40) 4.8	640 (A)	1.5 (A) \sim 1 (B)	i,z	24

^aThe number of spectroscopically confirmed members is in parentheses.

^bCapital letters are Johnson Filters and small case letters are Sloan filters.

^cDemarco et al. 2004

^dGirardi et al. 2004

3. The Clusters CL1252 and CL0152

CL1252

Figure 1 shows the center of one of our most distant clusters, CL1252 at $z = 1.237$. Spectroscopically confirmed members are marked with circles (passive galaxies) and squares (emission line galaxies). Figure 2 shows the confirmed cluster members in a combined i, z mosaic image of four overlapping ACS pointings. The two figures show several facts. The cluster is large; the most distant confirmed members are $\sim 170''$ (~ 1.4 Mpc) from the "center" of the cluster. Like other clusters at this redshift, the projected image of CL1252 is elongated. Finally, the passive, primarily early-type galaxies, are more strongly concentrated to the center and to the axis of the cluster than are the later type galaxies with $[\text{OII}]\lambda 3727$ emission, i.e. the star-forming galaxies. The X-ray and lensing results discussed below show that the early-type galaxies are primarily in the deepest part of the cluster's potential.

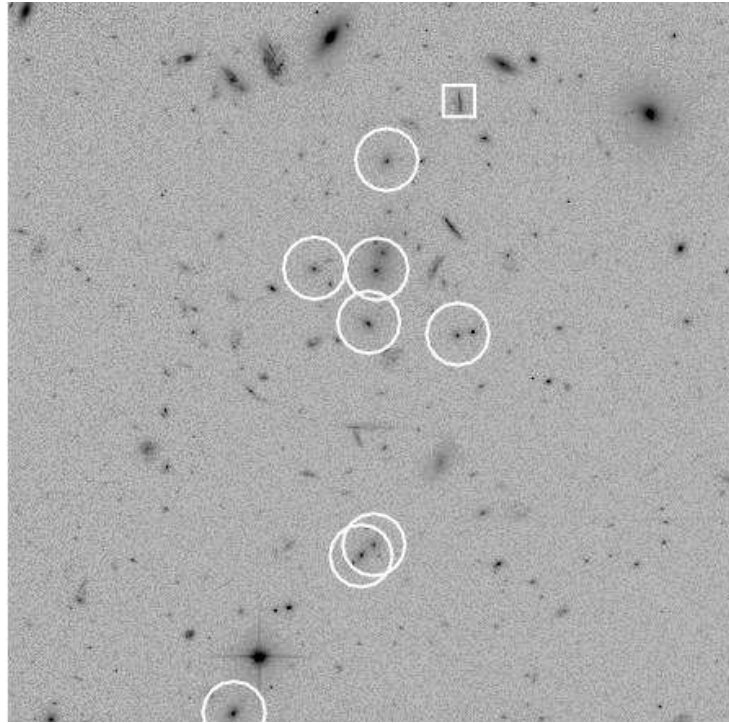


Figure 1. An ACS composite i, z image of the center of the cluster CL1252 at $z = 1.237$. The field is $70''$ square (~ 580 kpc in the restframe). Spectroscopically confirmed members are circled; emission line galaxies are boxed. The circles are $6''$ (50 kpc) in diameter. The "red" early-type cluster members are very conspicuous in a composite ACS i, z /VLT-K image.

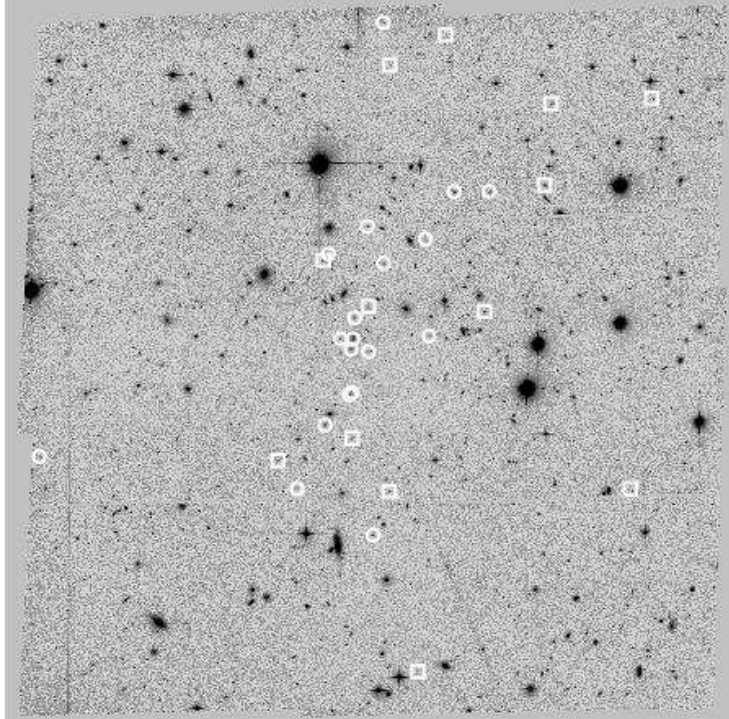


Figure 2. An ACS composite *i,z* mosaic image of four overlapping fields centered on CL1252 (symbols as in Figure 1). The field is $\sim 350''$ on a side (~ 2.9 Mpc in the restframe).

Figure 3 shows the spatial distribution of spectroscopically confirmed and photometrically selected galaxies in CL1252, along with a number of other clusters in our sample, coded by Hubble type. The figure, which is a visual representation of the morphology-density relationship (MDR), shows that E and S0 galaxies are concentrated along an axis, whereas the latter type galaxies have a much wider distribution. The MDR for six clusters is discussed at length in Section 1.4.

Figure 4 shows the observed ACS F775-F850LP color-magnitude (CM) relation for CL1252. The relation is quite tight and implies an intrinsic color scatter in these bandpasses of only 0.024 mag for the ellipticals, or 0.030 mag for all the early-type galaxies (ellipticals and S0s). Such a low scatter at this redshift when the universe was less than 5 Gyr old implies either a very high degree of synchronization in the formation of the stars in different galaxies (an unlikely scenario given the stochastic nature of hierarchical assembly), or that the galaxies are already advanced in age so that the fractional age differences are small. Given an assumed form of the star formation history, it is possible to derive the mean age of the galaxy population.

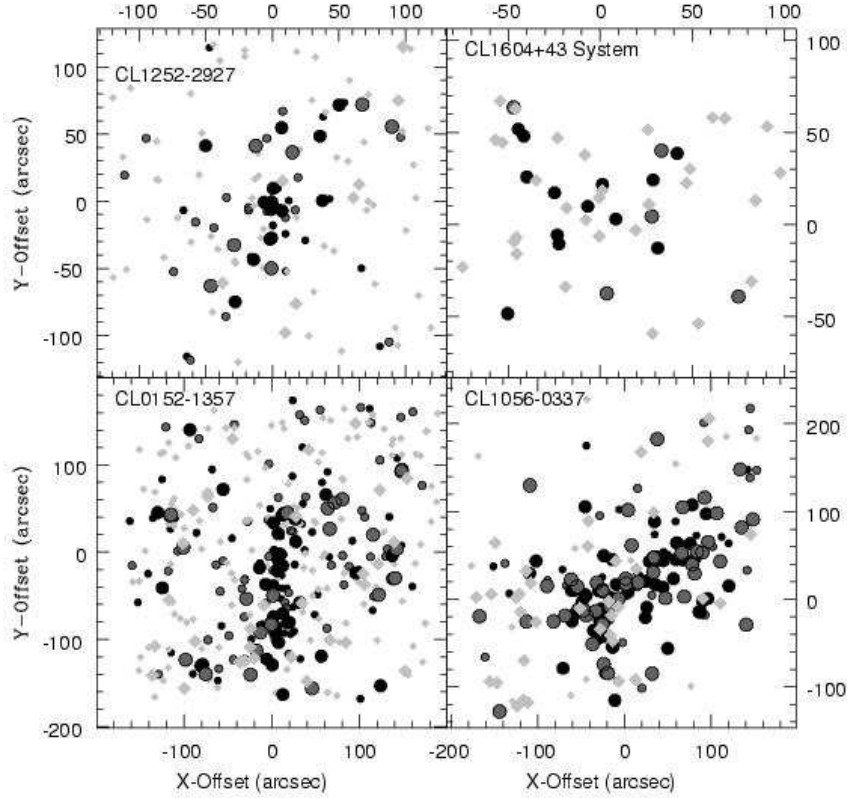


Figure 3. The spatial distribution of galaxy types in five clusters. Light grey diamonds are spirals, dark grey circles are S0s, and black circles are ellipticals. Large symbols are spectroscopically confirmed members and small symbols are candidate cluster members based on Bayesian photometric redshifts. Data for the two 16-hr clusters are combined into one plot.

We simulated the evolution in the observed galaxy colors using two simple star formation histories (Blakeslee et al. 2003: B03). In the first, the galaxies form in single bursts randomly distributed over the interval between the epoch of recombination and some ending time prior to the epoch at which the cluster is observed. In the second, the galaxies form stars at constant rates between randomly selected times prior to the epoch at which they are observed. The true star formation history is likely somewhere between the extremes of these single burst and constant formation models. The two models imply mean ages of 2.6 to 3.3 Gyr for the elliptical galaxies with a scatter in age of about 35%. This means that the stars in these galaxies formed over a period of about 1 Gyr, centered near a redshift of $z \approx 3$. The same models give a mean age of 1–2

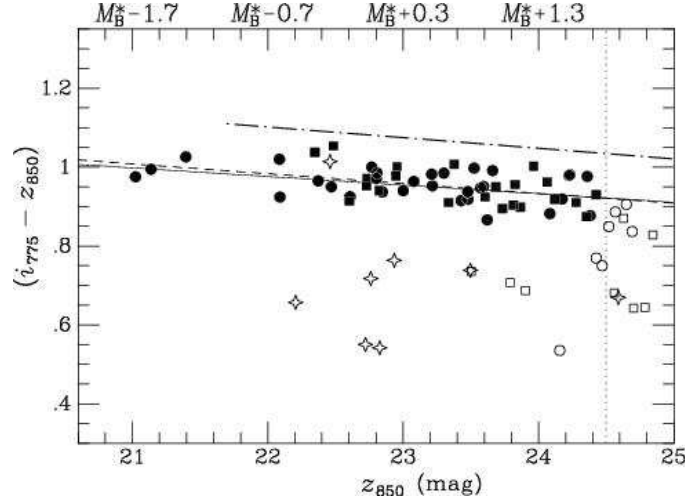


Figure 4. ACS color-magnitude diagram for confirmed members of the CL1252 cluster, and other early-type galaxies within a 2 arcminute radius of the cluster center (excluding spectroscopically known interlopers). Circles and squares represent elliptical and S0 galaxies, respectively. Solid symbols indicate galaxies that we use for fitting the slope and scatter of the CM relation, while open symbols (all of which lack spectroscopic information) were rejected as probable interlopers or as below the faint magnitude cutoff (indicated by the dotted line). Finally, the star symbols show 8 confirmed late-type members of the cluster, most of which are significantly bluer than the early-type CM relation. Two representative linear fits are shown: a fit to the 15 confirmed elliptical members (solid line) and to the 52 early-type red-sequence galaxies (including probable but unconfirmed members). The labels at top give the approximate luminosity conversion, assuming the WMAP cosmology and -1.4 mag of luminosity evolution, such that $M_B^* = -21.7$ (AB). The relation for the Coma cluster, transformed to these bandpasses at $z = 1.24$ (no evolution correction), is indicated by the dot-dashed line.

Gyr for the S0 population, with a scatter of $\sim 50\%$, and of course the blue colors and large scatter of the late-type galaxies imply ongoing star formation. These results are consistent with the features observed in the galaxy spectra. Thus, galaxies in protoclusters at $z \approx 3$ must have experienced very high rates of star formation, which declined sharply to the modest levels observed near $z \sim 1$. ACS observations of protocluster candidates at these high redshifts appear to be consistent with this view (Miley et al. 2004).

Lidman et al. (2004) come to very similar conclusions from their analysis of a CMD measured from deep VLT J,K_s images of CL1252. Using instantaneous single-burst solar-metallicity models, they conclude that the average age of galaxies in the center of CL1252 is 2.7 Gyrs.

Rosati et al. (2004a: R04) combined Chandra and XMM-Newton observations of CL1252 to measure the temperature, gas mass, metallicity, and bolometric luminosity of CL1252 within a $60''$ radius (500 kpc). Their results are

summarized in Table 2. The total mass in the last column is within a radius of 536 ± 40 kpc.

Table 2. X-ray Properties of CL1252.

$L_{[0.5-2.0]}$ $10^{44} \text{ erg s}^{-1}$	$L_{[Bol]}$ $10^{44} \text{ erg s}^{-1}$	T_X keV	Z_{gas} Z_{\odot}	M_{gas} $10^{13} M_{\odot}$	M_{tot} $10^{14} M_{\odot}$
$1.9^{+0.3}_{-0.3}$	$6.6^{+1.1}_{-1.1}$	$6.0^{+0.7}_{-0.5}$	$0.36^{+0.12}_{-0.10}$	$1.8^{+0.3}_{-0.3}$	$1.9^{+0.3}_{-0.3}$

The left hand panel of Figure 5 shows the projected distribution of the total mass in CL1252 derived by Lombardi et al. (2004:L04) from an analysis of the weak lensing in the ACS images. The middle panel shows adaptively smoothed X-ray contours from R04’s Chandra observations of the cluster. The right hand panel shows the smoothed VLT K-band light distribution of photometrically selected cluster members (Toft et al. 2004: T04). The centroids of the distributions of X-ray gas and galaxy light are very close to one another. The adaptively smoothed X-ray image shows an edge brightening on one side that suggests the gas and the brightest concentration of galaxies are moving in a direction parallel to the long axis of the cluster defined by its early-type galaxies (cf Figures 1, 2, and 3). If this interpretation is correct, the hot gas trapped in the deepest potential is interacting with a lower density gas associated with galaxies further down the axis of the cluster. However, the projected distribution of total matter is lagging rather than leading the compressed edge of the hot gas. Unless the mass distribution is being significantly affected by the mass associated with an obvious foreground cluster, this fact argues against a scenario wherein collisionless cold dark matter is leading hot gas that is retarded by pressure forces.

Despite its age of less than 5 Gyr, R04 conclude that CL1252 is well thermalized, with thermodynamical properties, as well as metallicity, very similar to those of clusters of the same mass at low redshift. Nonetheless, the elongation and large angular extent of the cluster, as well as the leading edge of the X-ray gas, suggest that it is still collapsing, with mergers and gas stripping of many of the galaxies yet in the future. The relatively high value of the metallicity is consistent with a scenario wherein the major episode of metal enrichment and gas preheating by supernovae occurred at $z \sim 3$.

CL0152

Figure 6 shows a composite ACS i,z image of the richest of two prominent subclusters in CL0152. Spectroscopically confirmed galaxies are circled. Figure 7 shows an overlay of Chandra X-ray contours on the entire ACS field. The hot gas is confined to two components that coincide with two concen-

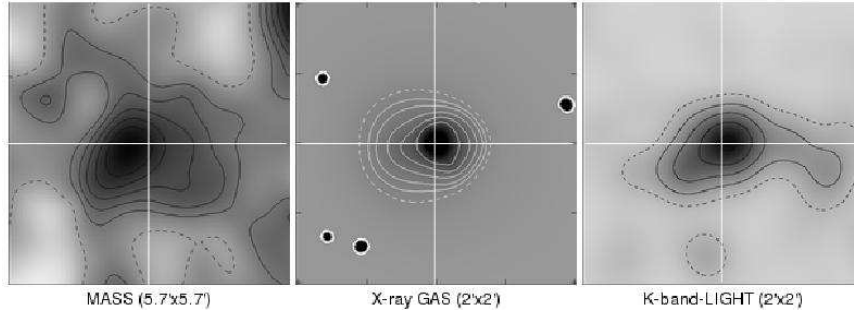


Figure 5. Mass, hot gas, and luminous matter in CL1252. The left panel is the projected mass distribution derived from L04's analysis of weak lensing in ACS images. The middle panel is the X-ray contours from adaptive smoothing of R04's Chandra observations of the cluster. The right panel is T04's smoothed K-band light distribution of photometrically selected cluster members. The images are rotated 90 degrees counter clock wise with respect to the images in Figures 1 and 2.

trations of early-type galaxies. As discussed below, the X-ray properties and mass distribution derived from our weak lensing analysis suggest that the two mass components are merging. Confirmed members with no emission lines are circled, and star-forming galaxies with $[\text{OII}]\lambda 3727$ emission are marked by "stars" (Homeier et al. 2004). The cluster is larger than the $\sim 350''$ (~ 2.7 Mpc) field of the four overlapping ACS exposures. The confinement of the star-forming late-type galaxies to a ring or shell around the two subclusters is very striking. Two bright X-ray sources in the field coincide with two galaxies that are confirmed members. One of the two galaxies is an isolated (barred) spiral. The other is a very "disturbed" spiral in a compact group of five galaxies, and appears to have had a recent close interaction with another galaxy. Images and spectra of the two galaxies are shown in 8. Both galaxies have broad MgII 2800 lines, showing that they are Seyferts (Demarco et al. 2004).

Jee et al. (2004: J04) used ACS images of CL0152 to measure the gravitationally induced shear in the weakly distorted background galaxies that fill the field around the cluster. The PSF of ACS has a complicated shape, which also varies across the field. J04 constructed the PSF model of ACS from an extensive investigation of 47 Tuc stars in sufficiently uncrowded regions. They verified that the model PSF accurately describes the *actual* PSF variation pattern in the cluster observations after a slight adjustment of ellipticity is applied.

Figure 9a shows the mass reconstruction created from the shear field with a maximum-likelihood algorithm overlaid on a smoothed luminosity distribution that is based on the spectroscopically confirmed cluster members. The mass map is dominated by the dark matter within the cluster. The correspondence between the mass map and the luminosity distribution is quite good. Figure 9b

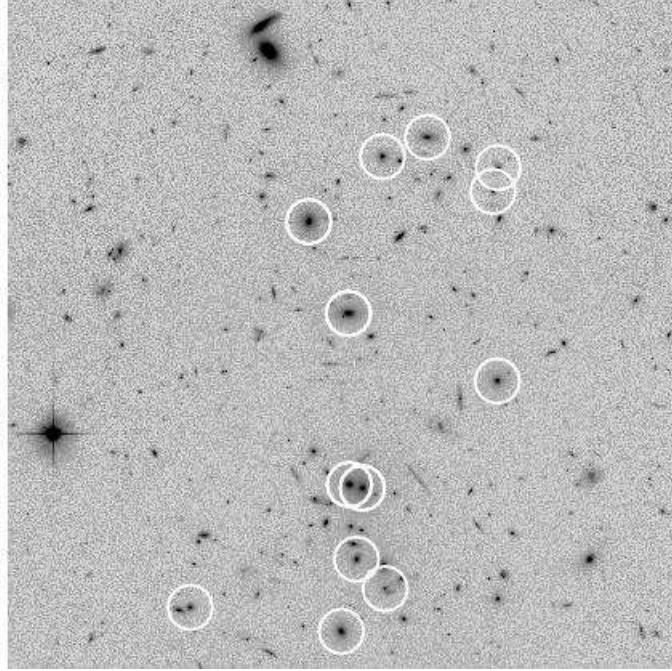


Figure 6. A composite ACS i,z image of the brighter of the two most conspicuous sub-clusters in CL0152. The field size is $90''$ (~ 690 kpc in the restframe). Spectroscopically confirmed members are circled ($6''$ diameter; ~ 50 kpc in the restframe). There are several thin arcs from lensed background galaxies that are much bluer than the early-type galaxies in the cluster. The lensed galaxy just below and to the left of the two overlapping circles has two components that are mirror images, indicating that the galaxy is very close to a caustic.

shows the smoothed X-ray contours derived from J04's reanalysis of archival Chandra observations. The figure shows that the peaks of the X-ray emission in the two brightest subclusters are lagging behind the peaks in the luminous matter and the dark matter. The displacement of the southern X-ray peak relative to the galaxies was noted by Maughan et al. (2003: M03). They suggested that the relatively collisionless galaxies are moving ahead of the gas. J04's (dark) mass and luminosity maps strengthen this suggestion. The two subclusters appear to be merging due to their mutual gravitational attraction. If the mass is cold dark matter, it is collisionless, whereas the merger of the hot gas in the two subclusters will be slowed by pressure forces. Further support for this picture comes from M03's suggestive evidence that there is a faint ridge of higher temperature gas midway between the two components and perpendicular to the long axis of the cluster.

In a standard Λ CDM cosmology, J04 find a mass of $1.92 \pm 0.3 \times 10^{14} M_{\odot}$ within a $50''$ radius (380kpc). This value agrees with M03's $2.4^{+0.4}_{-0.3} \times 10^{14} M_{\odot}$

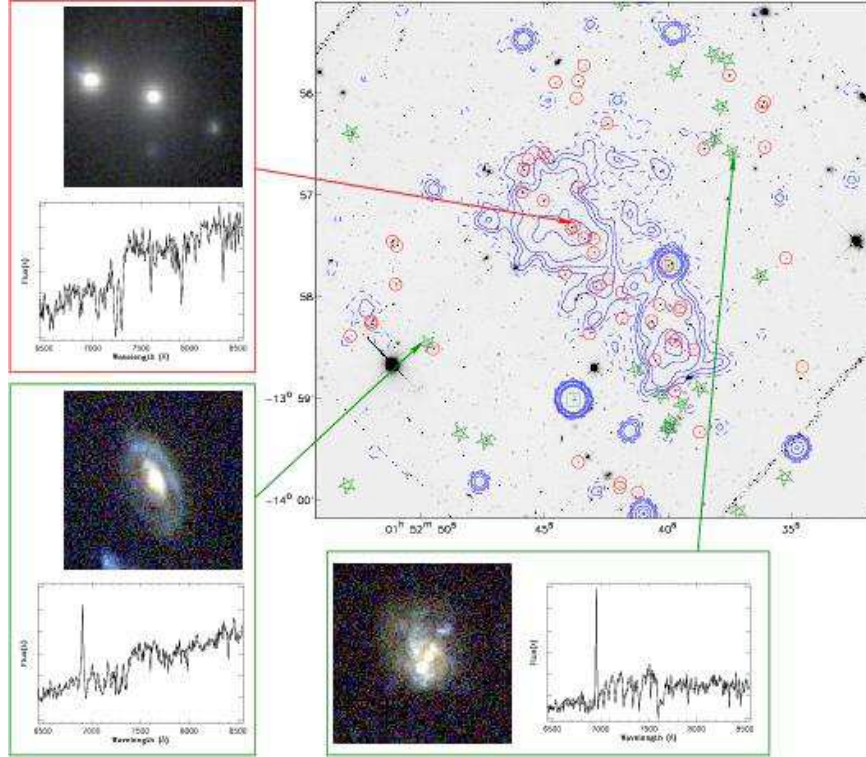


Figure 7. Star-forming galaxies in CL0152 and morphology of the X-ray emitting gas. Spectroscopically confirmed passive galaxies are circled and galaxies with star formation, as indicated by $[\text{OII}]\lambda 3737$ emission, are shown with a "star". The latter are typically spirals and late-type galaxies, while the former are mostly E/S0s. The insets show typical morphologies and spectra. The spatial segregation of the star forming later type galaxies is very striking. The Chandra X-ray isophotes (Demarco et al. 2004; Maughan et al. 2003) are 3, 5, 7, 10, 20 and 30 sigma above the background.

within the same radius derived from the Chandra X-ray observations. Transforming to $\Omega_M = 0.3$, $\Omega_\Lambda = 0.7$, $H_0 = 100$ for comparison with Joy et al.'s (2001: J01) Sunyaev-Zeldovich mass of $2.1 \pm 0.7 \times 10^{14} M_\odot$ within $65''$, J04 find $1.7 \pm 0.2 \times 10^{14} M_\odot$ for $r \leq 65''$, a value encompassed by J01's larger error bars.

In summary, the relatively high spatial resolution of J04's weak lensing mass distribution reveals several concentrations of mass that coincide with luminous substructure within the cluster. The offsets between the peaks in the X-ray emitting gas and the peaks in the dark matter provide evidence that the cluster components are merging. The mass derived from the weak lensing agrees with masses derived from the SZ effect and from the X-ray emission.

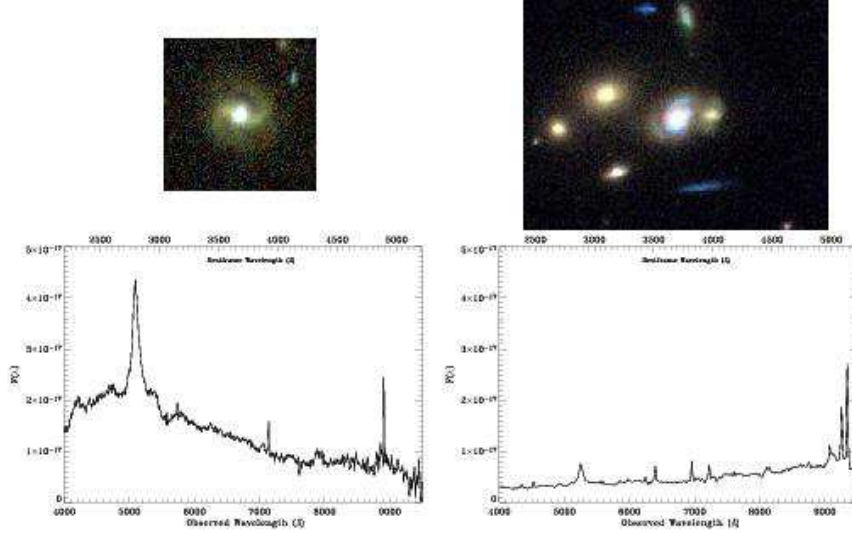


Figure 8. Two X-ray bright Seyfert galaxies in CL0152. The respective sizes of the left and right panels are $5'' \times 5''$ (38×38 kpc) and $10'' \times 7.5''$ (76×57 kpc). The AGN in the right hand panel is the brightest spiral and appears to be interacting with a fainter, smaller spiral. The projected separation of the two spirals is $1.15''$ (8.8 kpc). The strong broad emission line in each spectrum is MgII2800.

4. Global Properties of the Clusters

Cluster Morphology-Density Relation

The correlation between morphology and density is a fundamental characteristic of the local universe (Dressler 1980: D80; Postman & Geller 1984: PG83; Goto et al. 2003). The morphology-density relation (MDR) and its evolution are therefore essential predictions of any viable large-scale structure formation scenario. Dressler et al. (1997: D97) measured the MDR at $z \sim 0.4$ and concluded that the fraction of S0 galaxies has increased significantly over the past 4 Gyr, suggesting that these galaxies are relatively recent structures formed from later-type systems infalling into clusters. Smith et al. (2004: Sm04) used WFPC2 images of 6 clusters in the range $0.76 \leq z \leq 1.27$ (many of which are in common with our ACS survey) to obtain the first measurement of the MDR at look back times up to 8.8 Gyr. Sm04 find that the form of the MDR has undergone significant evolution particularly at the high density end where the early-type (E+S0) fraction has increased from 0.7 ± 0.1 at $\sim 10^3$ galaxies Mpc^{-2} at $z \sim 1$ to ≥ 0.9 at the present epoch. At low densities, very little evolution is detected. They propose a series of simple models to explain this trend and nearly all result in an early-type population at $z \sim 1$ in which S0 galaxies are quite rare (typically $\leq 10\%$ of the population).

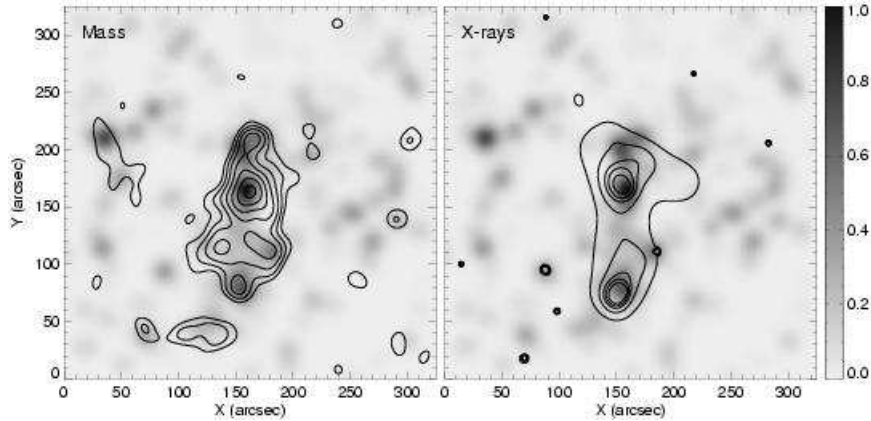


Figure 9. The left hand panel shows J04’s mass contours overlaid on the smoothed luminosity distribution derived from the i_{775} image. The map resolves five mass concentrations within the elongated main body of the cluster. There are an additional four mass concentrations outside the main body that are associated with confirmed cluster members. The right hand panel shows smoothed Chandra X-ray contours overlaid on the luminosity distribution. The hot gas is lagging behind the luminous and dark matter along and perpendicular to the axis of the cluster.

We visually classified the morphologies of all galaxies in each of our ACS images regardless of position or color. The morphological classification was performed on the full sample of $\sim 3,500$ galaxies brighter than 24 mag by one of us (MP) but 3 other team members classified a subset of 20% of these to provide an estimate of the uncertainty in the classifications. The classifications were done in the ACS band that samples at least part of the rest-frame B -band in each cluster. Unanimous or majority agreement between all 4 classifiers in the overlap sample was achieved for 75% of the objects brighter than $i_{775} = 23.5$. There is no significant systematic offset between the mean classification for the 3 independent classifiers and the classification by MP giving confidence that the full sample was classified in a consistent manner. MP also classified all galaxies from our ACS exposure of MS1358 ($z = 0.33$) that were in common with the extensive study performed by Fabricant et al. (2000). Agreement between the MP classifications and those from Fabricant et al. was achieved $\sim 80\%$ of the time with no systematic bias seen in the discrepant classifications.

We compute a projected density using the same prescription as D80, D97, and Sm04. For CL0152 and MS1054, we have a sufficient number of spectroscopic redshifts that we can compute the MDR just using confirmed members. We correct the measured density for incompleteness in our redshift survey and to match the same fiducial luminosity limit used by D80 - although we allow for evolution of the characteristic galaxy luminosity (e.g., Postman, Lubin, & Oke 2001). For CL1252 at $z = 1.24$, we derive the MDR using a photo- z

selected sample. We confirm that the photo- z derived MDR is not significantly different from the spectroscopic redshift result. We have corrected the densities for CL1252 for incompleteness and contamination due to the fact the scatter in the photometric redshifts is significantly larger than the cluster velocity dispersion. The MDR expressed as the early-type fraction (E+S0) as a function of local projected density is shown in Figure 9. We also show the MDR's derived for the current epoch (D80) and at $z \sim 1$ by Sm04. We find that our ACS-based MDR exhibits less evolution than the Sm04 result but is still significantly different from the current epoch MDR. The excellent angular resolution of ACS allows us to make a direct measurement of the S0 fraction. We find S0 fractions of 0.31 ± 0.10 and 0.19 ± 0.20 at $z = 0.83$ and $z = 1.24$, respectively. Both values are higher than the extrapolations made by Smith et al. based on the observed S0 fractions at $z = 0.5$. However, the difference is at best a 2 sigma result. Furthermore, the ACS data suggest a weak dependence of the S0 fraction on projected density that is similar to what is seen today. These S0 fractions are comparable with what D97 find at $z = 0.4$ but are less than the local S0 fraction, which is approaching 0.5–0.6 in cluster cores (D80, PG83, Poggianti 2001). If these results hold up as we extend our analysis to the entire cluster sample it would suggest an early ($z > 1.2$) formation of a 20–30% population fraction of lenticular systems that undergoes a doubling in population only in the past 4 Gyrs. One caveat is that the 3 clusters used in the analysis here are all relatively X-ray luminous systems – it remains to be seen if there is a significant correlation between X-ray luminosity and the rate at which the MDR evolves. A more thorough description of our MDR measurement will be discussed by Postman et al. (2004).

Brightest Cluster Galaxies

Studying the brightest cluster galaxies (BCGs) in our clusters can reveal essential clues to the timescales for their assembly process. The first significant difference is that 3 of the 6 BCGs are S0 or later. It is rare in current epoch clusters to find such a high fraction of BCGs with disks. In the clusters with later type BCGs, the process of galactic cannibalism may have either not yet begun or may only just be getting underway. We fitted the 2D surface brightness distributions of each BCG and used the best-fit model to measure the metric luminosity within a radius of 14.5 kpc ($h = 0.7$, $\Omega_m = 0.3$, $\Omega_\Lambda = 0.7$). The photometric measurements were transformed to the rest-frame AB B-band so that we could compare the data with Bruzual-Charlot predictions for a passively evolving early-type SED. We find that the BCGs in our clusters are, on average, less luminous than a passively evolving BCG normalized to match the mean current epoch BCG metric luminosity. The exception is the BCG for MS-1054, which is quite consistent with these predictions. This suggests that many of these BCGs will still undergo significant merger events. For example, the

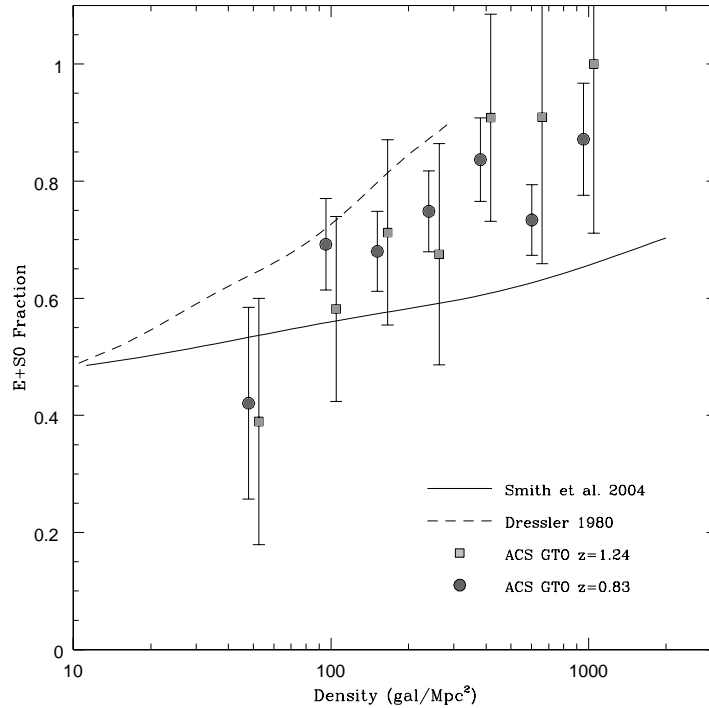


Figure 10. The morphology-density relation for two epochs: $z=0.83$ (7 Gyr ago) and $z=1.24$ (8.6 Gyr ago). The early-type fraction includes all galaxies classified as E or S0. Results from previous studies are shown for comparison. The Smith et al. (2004) result (based on WFPC2 imaging) covers a similar range of redshifts. We find a significantly higher fraction of S0 galaxies at both epochs compared to their extrapolation from $z=0.50$. We also see less evolution in the MDR than they report but we are not inconsistent with their result.

residuals after our best fit model for the BCG and 2nd-ranked in CL1252-29 are subtracted show substantial structure consistent with tidally stripped stars. These two galaxies are close together and thus appear to be in the process of merging. As the 2nd-ranked galaxy is nearly as luminous as the BCG, the luminosity of the final merger will be nearly double, making it comparable to the luminosity of a current epoch BCG. A further indication that BCGs at $z \sim 1$ are still assembling is that the difference between the 1st and 2nd-ranked luminosity within the above metric radius is on average only 0.09 mag (again the MS-1054 M2-M1 value is the outlier at 0.30 mag). Only 8% of current epoch BCGs have M2-M1 as small as 0.09 mag (Postman & Lauer 1995).

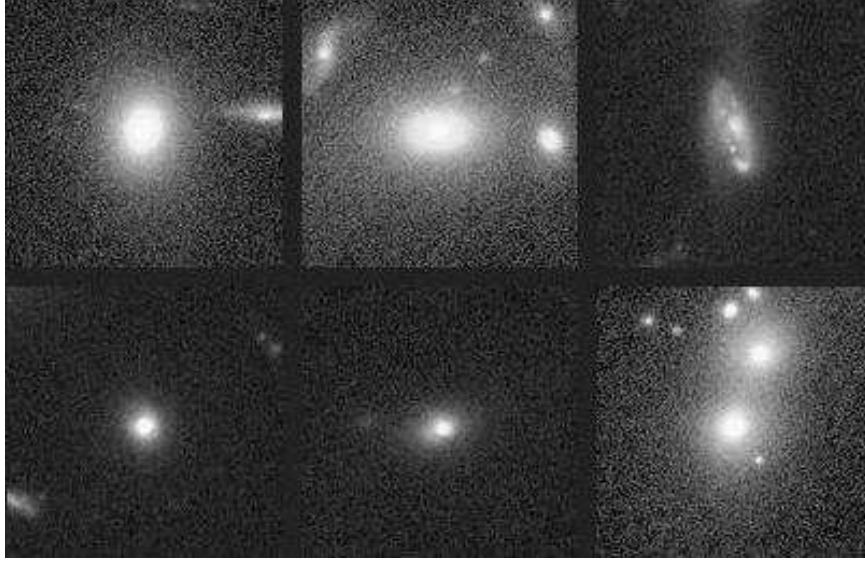


Figure 11. BCGs identified in 6 of our intermediate redshift clusters. From left to right in the top row: CL0152-13, MS1054-03, CL1604+4304. From left to right in the bottom row: CL1604+4321, CL0910+54, CL1252-29.

Table 3. Properties of the Brightest Cluster Galaxies in Six Intermediate Redshift Clusters.

Cluster	$RA(J2000)$ $Obs\ Color$	$DEC(J2000)$ ABB_{rest}	z_{obs} $(U-B)_{rest}$	Type $(M2 - M1)$	Obs Mag
MS1054	10:57:00.0	-03:37:36	0.8313	E	20.14 (i)
	1.58 (V-i)	-22.877	1.30	0.301 (i)	
CL0152	01:52:46.0	-13:57:00	0.8342	E	20.73 (i)
	1.22 (r-i)	-22.516	1.26	0.088 (i)	
CL1604+4304	16:04:25.0	+43:03:21	0.8966	Sb/c	20.89 (I)
	1.65 (V-I)	-22.497	1.15	0.027 (I)	
CL1604+4321	16:04:36.7	+43:21:41	0.9222	S0/a	21.31 (I)
	1.15 (V-I)	-22.236	0.73	0.009 (I)	
CL0910	09:10:45.7	+54:41:25	n/a	Sa?	21.52 (z)
	1.03 (i-z)	-22.337	1.18	0.174 (z)	
CL1252	12:52:54.4	-29:27:18	1.2343	E	21.30 (z)
	0.96 (i-z)	-23.046	1.22	0.121 (z)	

Color-Magnitude Diagrams

Figure 12 shows that a well defined "red sequence" appears to be a characteristic of all clusters at $z \sim 1$. Although we do not yet have final constraints on the ages based on the scatter in color for all these systems, the striking def-

initiation of the sequences suggests that, as with CL1252, we are observing the ellipticals in these clusters at an epoch when they are $\sim 3\text{--}4$ Gyr old.

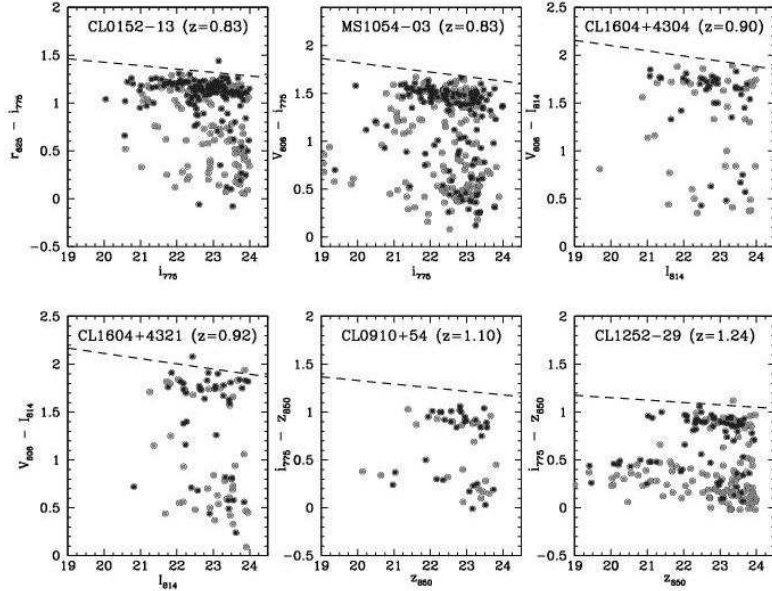


Figure 12. The CMDs for E and S0 galaxies along the line of sight to six $z \sim 1$ clusters. Ellipticals are dark grey and the S0s are light grey. The dashed line is where the Coma Cluster CMD would lie if Coma were simply redshifted to the relevant epoch and observed in the indicated passbands.

5. Discussion and Summary

Deep ACS and NICMOS images (this paper; van Dokkum et al. 2001) show that elliptical, S0, and spiral galaxies are present in clusters at redshifts up to $z \sim 1.3$. Analysis of the CMDs in clusters at $z \sim 1$ (B03, L04, van Dokkum & Stanford 2003, Holden et al. 2004) suggest that the cluster ellipticals underwent the bulk of their star formation 2.6 to 3.3 Gyrs earlier ($z \sim 3$). The morphology-density relation is well established at $z \sim 1$, with star forming spirals segregated in the outer parts of clusters and E/S0s concentrated in dense clumps. Thus, the properties of the majority of the luminous elliptical galaxies are well established. The one exception is that the magnitude difference, $M2 - M1$, between the second and first brightest galaxies in the clusters at $z \sim 1$ is smaller than in 93% of present-day Abell clusters.

In contrast, the spatial distribution of early-type galaxies in the $z \sim 1$ clusters is primarily elongated, often with two or more dense concentrations of galaxies (sub-clusters and groups). In general, the X-ray morphology follows

the galaxy concentrations, and, with the exception of MS1054, the X-ray emission is not spherical (Rosati 2004b: R04b). In some clusters the X-ray isocountours suggest interactions between sub-clusters (e.g. CL0152). There is evidence that the cluster bolometric X-ray luminosity L_X evolves from high to low redshift, but there is little evolution in the co-moving density (R04b). Finally, there appears to be mild evolution of the L_X vs T_X relation (Ettori et al. 2004), in disagreement with simple models. The combination of the two results suggests significant non-gravitational heating at earlier epochs.

When all of the facts are taken together, the following picture emerges. Clusters of galaxies are largely "in place" by $z \sim 1$, an epoch when the Universe was $\sim 40\%$ its present age. The early-type galaxies in these clusters, primarily found in high density regions, had largely ceased star formation by the time the Universe was 2.7 to 3.8 Gyrs old. The intracluster medium had already reached the metallicity of present-day clusters by $z \sim 1$ (Tozzi et al. 2003). The injection of metals from supernovae was likely one of the mechanisms that heated the gas in addition to adiabatic compression as the clusters collapse. This injection of heat "puffs up" the gas, which counteracts the expected cosmological evolution of the L_X vs T_X relation, yielding the mild evolution observed. The distribution of the hot gas and early-type galaxies is very similar in $z \sim 1$ clusters, suggesting that both have virialized in the center of the deepest potentials in the clusters.

In spite of the many similarities between $z \sim 1$ and present-day clusters, there are many significant differences. The distributions of the hot gas and the early-type galaxies are irregular and elongated rather than spherical. Thus, we appear to be observing the clusters at an epoch when they were still assembling from groups and sub-clusters. Support for this picture comes from the leading edge of the hot gas in CL1252 (R04) and from CL0152 (J04) where the gas appears to be lagging behind the luminous and dark mass in two merging sub-components. The BCGs appear to have considerable evolution ahead of them via mergers, for instance the two central galaxies in CL1252 appear ready to merge in the near future. Because spiral BCGs are rare in nearby clusters, the one in CL1604+4304 is likely to undergo morphological transformation or fade to lesser prominence as its gas is expended. The overall merging process will also result in the bolometric X-ray luminosities increasing as the $z \sim 1$ clusters evolve. In spite of a strong selection bias for the most luminous clusters, only one of our $z \sim 1$ clusters (MS1054) is brighter than R04b's fiducial $L_X^* \sim 3 \times 10^{44}$ ergs sec $^{-1}$. Using R04b's value for the evolution in luminosity, $L^* = L_0^*(1+z)^B$, with $B \sim -2.25$, the clusters will brighten by approximately a factor of 5 by the present epoch.

Many tasks remain for the future. We and others must fully characterize all of the clusters that are being studied with ACS, Chandra, XMM-Newton, and large ground based telescopes. Finally, we need to find clusters at earlier stages

of evolution between the present limit $z \sim 1.3$ and the apparent proto-clusters being studied at redshifts $z \geq 2$ (Miley et al. 2004).

Acknowledgments

ACS was developed under NASA contract NAS5-32865, and this research was supported by NASA grant NAG5-7697.

References

- Blakeslee, J., Franx, M., Postman, M., Rosati, P., Holden, B. P., et al. 2003, ApJ, 96, 143 (B03)
- Cole, S., Lacey, C., Baugh, C., & Frenk, C. 2000, MNRAS, 319, 168
- Demarco, R. et al. 2004, in preparation (D04)
- Dressler, A. 1980, ApJ, 236, 351
- Dressler, A., Oemler, A., Couch, W., et al. 1997, ApJ, 490, 577
- Ettori, S., Tozzi, P., Borgani, S., & Rosati, P. 2004, A&A, 417, 13
- Fabricant, D., Franx, M., & van Dokkum, P. 2000, ApJ, 539, 577
- Ford, H.C. et al. 2002, Proc. SPIE, 4854, 81
- Gioia, I. & Luppino, G. 1994, ApKS, 94, 583
- Girardi et al. 2004, in preparation
- Gunn, J.E., Hoessel, J.G., & Oke, J.B. 1986, ApJ, 306, 30
- Holden, B., Stanford, S. A., Eisenhardt, P. & Dickinson, M. 2004, AJ, 127, 2484
- Homeier, N. et al. 2004 in preparation
- Jee, J. et al. 2004, in press
- Joy, M., et al. 2001, ApJ, 551, L1
- Lidman, C., Rosati, P., Demarco, R., et al. 2004, A&A, 416, 829 (L04)
- Lombardi et al. 2004, in preparation
- Maughan, B. J., Jones, L. R., Ebeling, H., Perlman, E., Rosati, P., et al. 2003, ApJ, 587, 589
- Miley et al. 2004, this conference proceedings
- Poggianti, B. 2001, MmSAI, 72, 801
- Postman, M., & Geller, M. 1983, ApJ, 281, 95
- Postman, M., Lubin, L., & Oke, J. B. 2001, AJ, 122, 1125
- Postman, M., et al. 2004, in prep
- Postman, M., & Lauer, T. 1995, ApJ, 440, 28
- Rosati, P., Della Ceca, R., Norman, C., & Giacconi, R. 1998, ApJ, 492, L21
- Rosati, P., Tozzi, P., Ettori, et al. 2004a, AJ, 127, 230
- Rosati, P. 2004b, Carnegie Obs. Astro. Ser. 3: Clusters of Galaxies: Probes of Cosmological Structure and Galaxy Evolution, ed. J. Mulchaey et al. (Cambridge: Cambridge Univ. Press)
- Smith, G., Treu, T., Ellis, R., Moran, S., & Dressler, A. 2004, astro-ph/0403455
- Toft et al. 2004, A&A, in press, astro-ph/0404474
- Tozzi, P. et al. 2003, ApJ, 593, 705
- van Dokkum, P. G., Stanford, S. A., Holden, B. P., et al. 2001, ApJ, 552, L101
- van Dokkum, P. G. & Stanford, S. A. 2003, ApJ, 585, 79